Generating variable birdsong syllable sequences with branching chain networks in avian premotor nucleus HVC

Dezhe Z. Jin*

Department of Physics, The Pennsylvania State University, University Park, Pennsylvania 16802, USA

(Received 22 June 2009; revised manuscript received 14 August 2009; published 5 November 2009)

Songs of songbird species such as Bengalese finch consist of sequences of syllables. While syllables are temporally stereotypical, syllable sequences can vary and follow complex, probabilistic transition rules. Recent experiments and computational models suggest that a syllable is encoded in a chain network of projection neurons in premotor nucleus HVC (proper name). Precisely timed spikes propagate along the chain, driving vocalization of the syllable through downstream nuclei. However, the neural basis of the probabilistic transitions between the syllables is not understood. Here we propose that variable syllable sequences are generated through spike propagations in a network in HVC in which the syllable-encoding chain networks are connected into a branching chain pattern. The neurons mutually inhibit each other through the inhibitory HVC interneurons, and are driven by external inputs from nuclei upstream of HVC. At a branching point that connects the final group of a chain to the first groups of several chains, the spike activity selects one branch to continue the propagation. The selection is probabilistic, and is due to the winner-take-all mechanism mediated by the inhibition and noise. The transitions between the chains are Markovian. If the same syllable can be driven by multiple chains, the generated syllable sequences are statistically described by partially observable Markov models. We suggest that the syntax of birdsong syllable sequences is embedded in the connection patterns of HVC projection neurons.

DOI: 10.1103/PhysRevE.80.051902 PACS number(s): 87.18.Sn, 84.35.+i, 05.45.Xt

I. INTRODUCTION

Sequence is a fundamental aspect of many animal and human behaviors. Behavioral sequences are often variable but not random, and can be described by some "action syntax," similar to grammar in language [1]. Although numerous experimental and theoretical works on human and nonhuman primates performing instructed simple serial movements have provided some insights into the neural basis of action sequences [2–6], it remains unexplored how neural activity generates complex action syntax.

The songbird is an excellent model system for studying action sequences. Birdsong is a learned vocalization that has many parallels with human language [7–12]. Many songbirds sing songs with complex syntactical structures [13]. Figure 1 shows the song of a Bengalese finch as an example. The song consists of syllables—temporally stereotypical bursts of sounds separated by silent intervals. There are several distinctive syllables, which are labeled with letters on top of the spectrogram of the song [Fig. 1(a)]. The syllable sequence can be described by a transition rule that allows a syllable to be followed by another one chosen with some probability from a restricted set of syllables [13–18] [Fig. 1(b)]. Such a rule is rudimentarily similar to how words can be strung together with restricted flexibility in language [19], and allows generation of an unlimited number of distinctive syllable sequences.

The production of birdsong is controlled by the song system that consists of a set of brain nuclei linked to form a mostly feed forward excitatory pathway [20–23], as illustrated in Fig. 2. The premotor nucleus HVC (proper name) plays a key role in the song system. HVC projects to RA (the robust nucleus of the arcopallium). RA, in turn, projects to a hypoglossal motor nucleus containing motor neurons innervating the syrinx—the vocal organ of birds. HVC and RA are necessary for song generation, and form a premotor pathway in the song control system [20,21]. HVC is also a site of sensorimotor integration: it gets auditory input from NIF (the nucleus interfacialis of the nidopallium) [24–28]; it also gets input from UVA (the nucleus uvaeformis), a thalamic nucleus [21,29–31]. HVC has a rich internal structure [32–36]. There are at least three types of neurons: HVC(RA) neurons, which project to RA; HVC(X) neurons, which project to area X; and inhibitory interneurons [HVC(I) neurons], which do not project out of HVC. There are extensive connections between these neurons [36].

To date, most birdsong studies have been done on zebra finch [34,37–42], whose song consists of several repetitions of a motif, which is a fixed sequence of a few syllables [12]. Recordings in RA and HVC in singing zebra finches revealed that neurons in RA and in HVC have very different spiking patterns [37,40,43]. RA neurons that project to motor areas spike reliably with precise timings relative to acoustic features of the motif [37,43]. An RA neuron bursts about ten times during a motif. Different combinations of RA neurons burst at different times, driving different spike patterns in the motor neurons to generate varying acoustic features [37,43]. In contrast, HVC(RA) neurons have ultrasparse spiking patterns [40]. An HVC(RA) neuron bursts only once during a song motif. The burst typically lasts about 6 ms, emitting three to seven spikes, and has a precise timing relative to the motif. Different HVC(RA) neurons burst at different times. Thus, HVC(RA) neurons burst sequentially and form a sequencer that drives different combinations of RA neurons at different times [40,44,45]. An RA neuron bursts several

*djin@phys.psu.edu

 ©2009 The American Physical Society

FIG. 1. Spectrogram (a) and syllable transition diagram (b) of a Bengalese finch song. The syllables (I, A-G) are labeled on top of the spectrograms. Data courtesy of Alexay Kozhevnikov.

times during the motif since it is driven by different HVC(RA) neurons that burst at different times. These experiments show that, whereas RA neurons encode moment-to-moment patterns directly involved in producing the acoustic features of the song, HVC(RA) neurons encode the sequence and timing of these features [44,45]. The sequential structure of zebra finch song is thus reflected in the sparse sequential bursts of HVC(RA) neurons [40], which can be thought of as encoding the song syntax of zebra finch. Since an HVC(RA) neuron bursts once during the motif, the set of neurons firing during each syllable is distinctive.

A recent experiment showed that cooling HVC of a zebra finch during singing slows down the song uniformly in all time scales, supporting the idea that the sequential firings of HVC(RA) neurons are generated within HVC [46]. Computational models [47,48] proposed that such a firing pattern is produced by spike propagation in a synfire chain network, in which successive groups of HVC(RA) neurons are chained by unidirectional excitatory connections [49,50]. Chaining is the simplest network structure that can generate sparse, sequential firing pattern, and has been suggested as a neural mechanism for sequential order in general [49–55]. The microcircuit of HVC [36] allows the possibility that HVC(RA) neurons are organized into a chain network, because HVC(RA) neurons have excitatory connections with each other. The inhibitory interneurons are excited by HVC(RA) neurons, and also send inhibitory connections to HVC(RA) neurons, providing a local feedback inhibition to HVC(RA) neurons. Thus, the burst sequence in HVC could be produced through spike propagation along the excitatory connections between HVC(RA) neurons and regulated by the feedback inhibition via the interneurons. Such chain networks could arise during the development through a simple activity-driven self-organizing process [56].

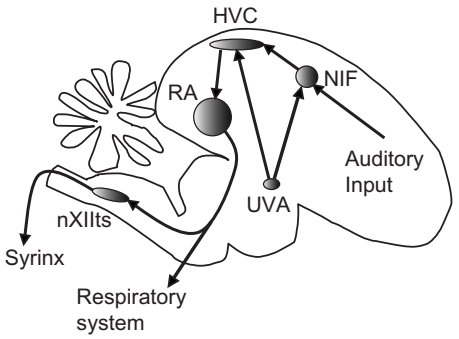

FIG. 2. Key brain nuclei of the song control system. Major projections in the motor pathway are indicated. Arrows indicate directions of projections, which are all excitatory.

Despite of the insights obtained from the studies of zebra finch, it remains a mystery how the variability of syllable sequences in songs of many other species such as Bengalese finch is produced. The simplicity of zebra finch song makes it unsuitable for studying song syntax with complex transition rules.

In this paper, we advance a "branching chain network" hypothesis of complex song syntax. It is a simple extension of the synfire chain model of the song sequence generation in zebra finch. We hypothesize that HVC is the site where the syntax of birdsong is generated. Each syllable is driven by spike propagation along a chain network of groups of HVC(RA) neurons unidirectionally connected through the excitatory synapses. The spike activity is aided by external inputs from UVA and/or NIF. The end of one chain is connected to the beginnings of several other chains to form a branching chain network. The transitions between syllables are governed by selective propagation of activity to one of the connected chains at a branching point. The selection is probabilistic, and is enforced by the mutual inhibition between the chains mediated by the inhibitory interneurons. The selection probability can be affected by auditory feedback through NIF. A schematic of how HVC(RA) neurons are connected to encode the syntactical rule of syllable A transitioning to either syllable B or C is shown in Fig. 3.

A prominent feature of our hypothesis is the winner-take-all selection of a chain at a branching point for the spikes to

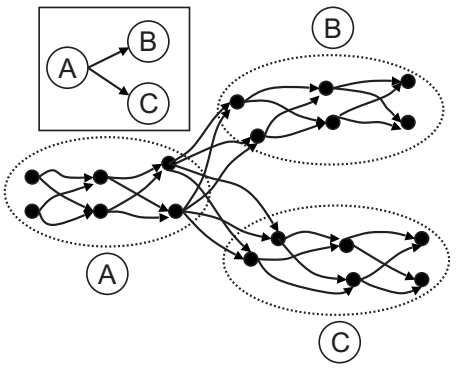

FIG. 3. A network of HVC(RA) neurons for generating a probabilistic transition from syllables A to B or C. Each syllable is encoded by a chain network. Chain A branches into chains B and C. HVC(RA) neurons inhibit each other through the interneurons (not shown). Spike activity propagates from chain A to either chain B or C but not both. The selection of B or C is probabilistic.

propagate. The spike activity must not decay or propagate simultaneously in more than one chain. A key theoretical issue is whether this mechanism is robust to noise and can be realized without delicate tuning of the network parameters. The issue has been addressed recently by Chang and Jin using chain networks of simple leaky integrate-and-fire neurons [57]. However, the robustness remains to be demonstrated when more realistic models of HVC neurons are used. Another important issue is how the transition probabilities are controlled. These, along with testable predictions of the hypothesis, are investigated through numerical simulations of biologically motivated model of the branching chain networks in HVC.

II. METHODS

A. Neuron models

HVC(RA) neurons have been studied in a number of experiments. Extracellular recordings in zebra finch during singing demonstrated that HVC(RA) neuron emit stereotypical bursts of three to seven spikes [40]. Intracellular recordings that injected currents to the somata of HVC(RA) neurons did not observe such burst activity [32–34]. Some of these recordings showed that HVC(RA) neurons have strong spike frequency adaptation [32], while others did not [33]. A recent experiment suggests that the adaptation is not prominent (Long, Jin, and Fee, submitted). Currently, detailed studies of the ion channels on HVC(RA) neurons are not available. We therefore construct a minimal model of HVC(RA) neuron that is consistent with the extracellular and intracellular recordings, with necessary ion channels commonly used in conductance based neuron models [47].

A key issue in modeling HVC(RA) neuron is the origin of the stereotyped bursts observed in the extracellular recordings. One possibility is that the bursts are generated through convergent inputs to HVC(RA) neurons from other HVC(RA) neurons and regulated by feedback inhibition through the interneurons [48,58]. However, such a network based mechanism requires fine tuning of the connection strengths between neurons to achieve the level of stereotypy of the HVC(RA) bursts observed in the experiments, especially with noise (Long, Jin, and Fee, submitted), thus is not robust [47].

Another possibility is that HVC(RA) neuron has an intrinsic cellular mechanism for burst generation [47]. A minimum model consistent with the experiments is a two-compartment model with a dendrite and a soma [47]. The soma has no bursting property, in agreement with the intracellular recordings. The dendrite is capable of generating calcium spike. When the membrane potential of the dendrite reaches a threshold, a high threshold Ca^{++} conductance is activated, leading to rapid depolarization of the dendrite due to the Ca^{++} current. Elevated calcium concentration, in turn, activates the calcium-dependent K^+ current, which leads to repolarization of the membrane potential. These nonlinear processes produce a stereotypical profile of the dendritic membrane potential, which drives stereotypical burst of sodium spikes in the soma. The two-compartment model greatly enhances the robustness of burst propagation through

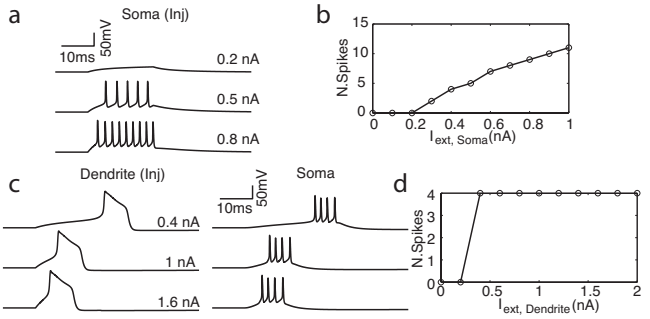

FIG. 4. Properties of two-compartment HVC(RA) neuron model. (a) Membrane potentials of the soma with three levels of step current injections to the soma of 20 ms long. (b) Number of spikes as a function of the level of the step current. (c) Membrane potentials of the dendritic compartment (left) and somatic compartment (right) under three levels of current injections at the dendritic compartment. (d) Number of spikes in the somatic compartment as a function of the level of the injected step current at the dendritic compartment.

synfire chain networks of HVC(RA) neurons [47]. Calcium spikes have been observed in mammalian hippocampal and cortical neurons, as well as cerebellar Purkinje neurons [59,60]. A recent experiment that coupled intracellular recordings with pharmacological manipulations supports the existence of calcium spikes in HVC(RA) neurons (Long, Jin, and Fee, submitted).

In the previous version of the two-compartment model of HVC(RA) neuron, a low-threshold potassium (KLT) conductance was incorporated in the soma to produce strong spike frequency adaptation and control the burst duration [47]. The recent experiment (Long, Jin, and Fee, submitted) indicates that the adaptation is not as strong as previously thought [32], and the burst duration is controlled by the calcium spike. We therefore modified the model and adjusted parameters to match these recent observations. Specifically, the somatic compartment of the HVC(RA) neuron model contains a leak conductance and Na^+ and delay-rectified K^+ conductances for action potential generation. The dendritic compartment contains a leak conductance and a high threshold Ca^{++} conductance plus a calcium-activated K^+ conductance for generation of a calcium spike in the dendrite. The two compartments are connected Ohmically. A calcium spike in the dendrite leads to a stereotypical burst of sodium spikes in the soma. In Fig. 4, we show the properties of the model neuron. Step current injection to the soma leads to spike response with the spike frequency proportional to the strength of the inject current [Figs. 4(a) and 4(b)]. Suprathreshold current injection to the dendrite produces stereotypical calcium spike regardless of the current strength, leading to stereotypical somatic spikes [Figs. 4(c) and 4(d)].

The HVC(I) neuron is modeled as a single compartment neuron that contains Na^+ and delay-rectified K^+ conductance for action potential generation, leak conductance, and high threshold K^+ conductance for enhancing fast spike generation. Under current injection, the interneuron spikes with high frequency, as shown in Fig. 5. Fast spiking is the hallmark of the HVC(I) neurons [32–34].

The mathematical details of the neuron models are described in Appendix.

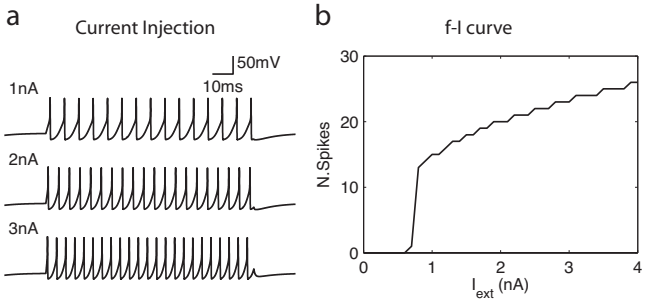

FIG. 5. Properties of the HVC(I) (inhibitory) neuron. (a) Membrane potentials of the neuron under three levels of injected step currents of 100 ms long. The area of the neuron is assumed to be 6000 μm^2. b. Number of spikes as a function of the level of the injected step current.

B. Network connectivity

Each chain consists of 20 groups of 60 HVC(RA) neurons. There are 1000 HVC(I) neurons. An HVC(RA) neuron connects to an HVC(I) neuron with a probability 0.05 and an excitatory synaptic conductance randomly chosen from 0 to G_{EImax}=0.5 mS/cm^2; an HVC(I) neuron connects to an HVC(RA) neuron with a probability 0.1 and an inhibitory synaptic conductance randomly chosen from 0 to G_{IEmax}. An HVC(RA) neuron connects to an HVC(RA) neuron in the next group, with an excitatory conductance randomly selected from 0 to G_{EEmax}. The connectivity of the network is shown in Fig. 6. The synaptic connections to the HVC(RA) neurons are made onto the dendritic compartments.

C. Noise and spontaneous activity

Noisy fluctuations of membrane potentials are induced in both HVC(RA) and HVC(I) neurons by applying noise spike trains generated with Poisson process. At each noise spike, a synaptic conductance randomly selected from 0 to G_{Noise} is added to either excitatory or inhibitory conductance with a probability 0.5. An HVC(RA) neuron receives noise spike trains of frequency 200 Hz and G_{Noise}=0.045 mS/cm^2 at the somatic compartment and noise spike trains of frequency 200 Hz and G_{Noise}=0.035 mS/cm^2 at the dendritic compartment. This leads to fluctuations of the membrane potentials in both compartments with a standard deviation about 3 mV. An HVC(I) neuron receives a noise spike train of frequency 500 Hz and G_{Noise}=0.45 mS/cm^2. This leads to spontaneous firing of HVC(I) neurons at about 10 Hz. The noisy fluctuations of the membrane potentials of neurons are shown in Fig. 7.

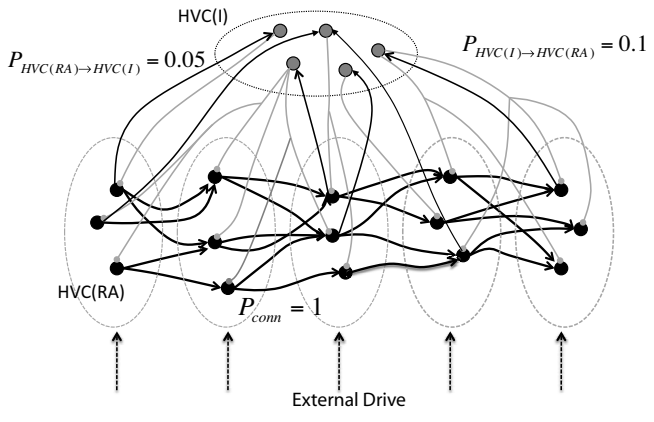

FIG. 6. Circuit diagram. HVC(RA) neurons (black circles) form successive group. An HVC(RA) neuron connects to all HVC(RA) neurons in the next group. An HVC(RA) neuron connects to an HVC(I) neuron (gray circles) with a probability 0.05; and an HVC(I) neuron connects to an HVC(RA) neuron with a probability 0.1.

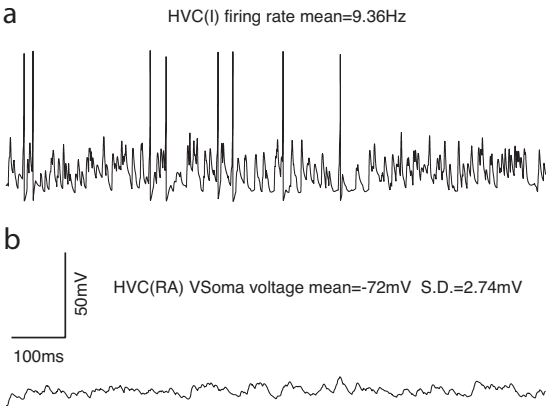

FIG. 7. Spontaneous activity of an interneuron (a) and an HVC(RA) neuron (b).

D. External drive

External inputs to HVC(RA) neurons are modeled as excitatory spikes generated by a Poisson process of frequency 1000 Hz. The synaptic conductance at each spike is randomly selected from 0 to $G_{ext,max}$, typically 0.05 mS/cm^2 unless specified otherwise.

III. RESULTS

To show that our branching chain network can generate complex variable syllable sequences, we simulated a network consisting of 4800 HVC(RA) neurons and 1000 HVC(I) neurons. The connectivity between HVC(RA) neurons and HVC(I) neurons are as shown in Fig. 6. The inhibitory conductance from an HVC(I) neuron to its connected HVC(RA) neuron is randomly selected from 0 to G_{IEmax} =0.4 mS/cm^2. The HVC(RA) neurons form four chain networks that drive syllables A, B, C, and D, respectively. There are 20 groups in each chain, and 60 neurons in each group. A neuron is connected to all neurons in the next group in the chain, with the conductance randomly selected from 0 to G_{EEmax}=0.3 mS/cm^2. The connections between the chains are set up such that the syntax of the syllable transitions is as given in Fig. 8(a). The syntax is similar to that of a real Bengalese finch, as shown in Fig. 1, with repeats of syllables and multiple permitted transitions from a given syllable. Specifically, syllable A can repeat itself or transition to B; B can repeat itself or transition to C or D; C transitions to D; D can transition to either A or C. The connections between the

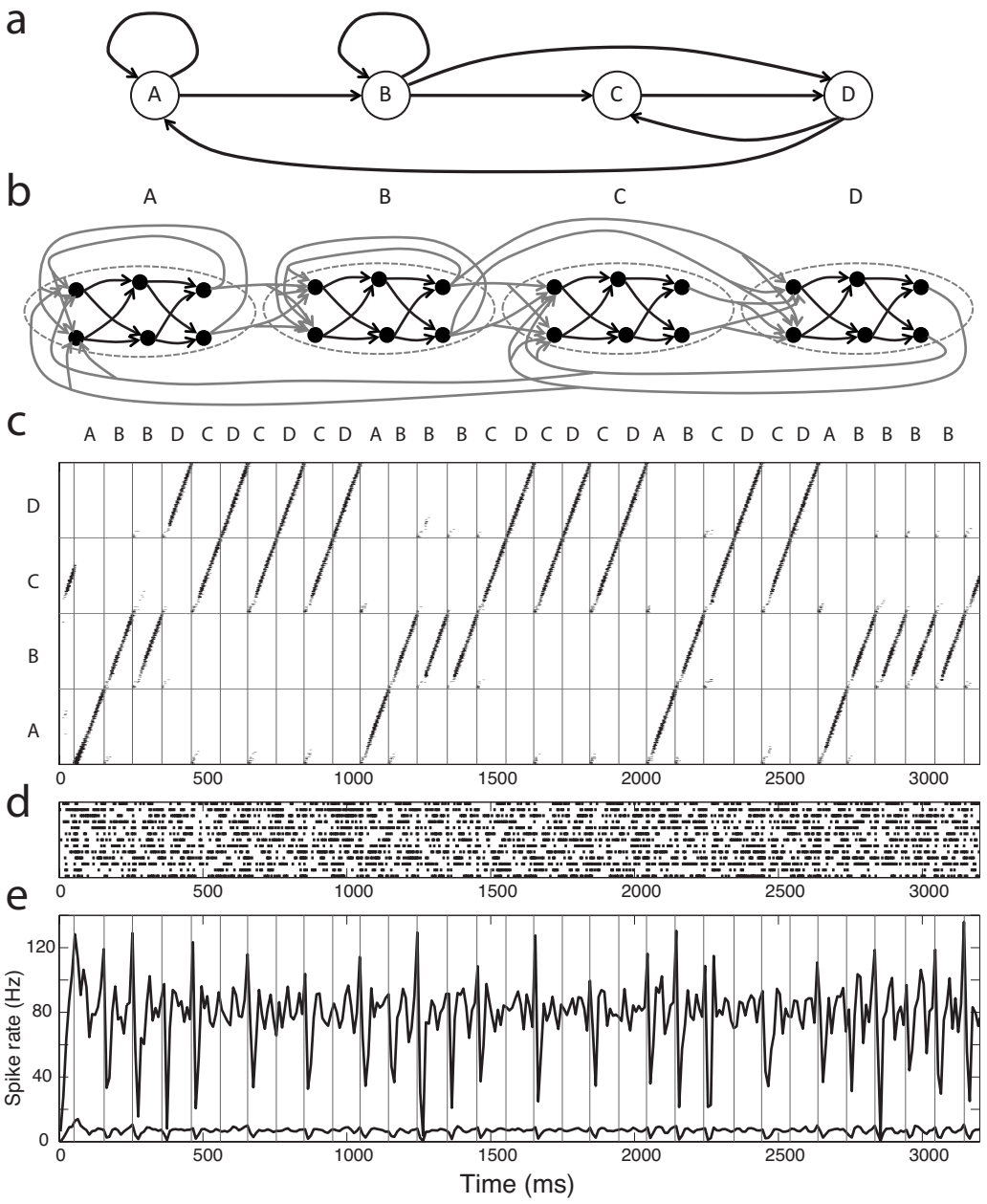

FIG. 8. The spiking dynamics of a branching chain network generating a variable song syntax. (a) The syntax of the syllable sequences. The possible transitions between syllables A,B,C,D are indicated with the arrows. (b) The schematics of connectivity of the branching chain network of HVC(RA) neurons. The inhibitory interneurons are not shown. Each syllable is encoded by a chain network, indicated by the black circles connected with the black arrows. The end of a chain network is connected (gray arrows) to the beginning of another chain (or itself) if there is a transition between the corresponding syllables. (c) The spikes of HVC(RA) neurons during one run of the dynamics. Neurons are ordered according the chains and groups in the chains. The vertical gray lines indicate the start of the dynamics at the branching points. The generated syllable sequence is on the top. (d) Spikes of the inhibitory interneurons. (e) The population averaged spike rates of HVC(RA) neurons (lower curve) and the interneurons (upper curve).

chains are set up accordingly. The neurons in the final group of the chain encoding syllable A (chain A) are connected to the neurons in the first groups in both chain A and chain B, reflecting the A to A or A to B transitions allowed by the syntax; the end of chain B is connected to the first groups of chains B, C, and D; so on and so forth. This leads to a branching chain network with the connectivity between the chains exactly following the transition diagram between the syllables, as shown in Fig. 8(b). The connection strength from a neuron in the last group to those in the first group are randomly selected from 0 to $G_{EEmax}=0.3$ mS/cm^2.

The spiking dynamics of the network is capable of generating variable syllable sequences that obey the specified syntax. This is shown in Fig. 8(c), in which we plot the spike raster of HVC(RA) neurons in a run of the dynamics. The neurons are ordered according to the group orders in the chains. At the beginning of the trial, spontaneous spike propagation appears in chain C due to the random external

inputs to the HVC(RA) neurons, which were present from $t=0$ ms. At $t=50$ ms, the neurons in the first group of chain A are induced to spike by injection of suprathreshold currents. This induces burst propagation along chain A, producing syllable A. Spikes of the final group of chain A activates the first groups of both chain A and B. Spikes weakly and briefly propagate on both chains (approximately 20 ms), but selects chain B for further propagation. After reaching the end of chain B, spikes briefly propagate on chains B, C, and D but choose chain B to propagate further. Such brief coactivation followed by selection of a single chain continues, generating a syllable sequence ABBDCDCDCDABBBCDCDCDABCDCDABBBB over a period of 3.2 *s*. The sequence obeys the syllable transition rule.

An HVC(RA) neuron bursts once during spike propagation in a single chain because of the chain connectivity. In contrast, HVC(I) neurons spike throughout the entire trial, as shown in Fig. 8(d), because HVC(I) neurons are excited by randomly selected neurons in all chains. The population spike rate of HVC(I) neurons tends to increase and decrease during the brief coactivation periods, as shown in the upper curve in Fig. 8(e). The increase reflects the simultaneous activation of several groups in multiple chains. The resulting increased inhibition reduces the population activity of HVC(RA) neurons [the lower curve in Fig. 8(e)], which in turn decreases the HVC(I) activity. After this competing period, spike steadily propagates in a single chain.

In our model, a syllable is driven by a chain network in HVC. It is crucial that a single chain is selected after a transient period at a branching point, which is accomplished by mutual inhibition between the chains. The inhibition should be sufficiently strong for this purpose. However, strong inhibition tends to stop spike propagation altogether, which should not be allowed either. Strong excitation between HVC(RA) neurons can counteract the inhibition to sustain the activity; however, the excitation should not be too strong, otherwise activity can propagate in multiple chains. This suggests that the excitation and inhibition strengths should be in a restricted regime. To show that our mechanism does not require a delicate tuning of the excitation and inhibition strengths, we simulated a network consisting of two chain networks that drive syllables A and B, respectively. The chains are connected to allow transitions from A to A or B, and from B to A or B, as shown in Figs. 9(a) and 9(b). We systematically varied the excitation strength G_{EEmax} and the inhibition strength G_{IEmax}. For each pair of parameters, we simulated the dynamics 40 times, each for 300 *ms*. The results are shown in Fig. 9(c). There are four regimes in the parameter space. When the excitation is too large, the spike activity is unstable. When excitation is moderate but still large compared to the inhibition, spike simultaneously propagates in both chains after the branching point from chain A to chains A and B. When the excitation is much weaker than the inhibition, spike propagation is not possible. The working regime, in which spike propagation selects either chain A or B after the branching point is between the regimes for simultaneous propagation and the random activity. The regime is quite large, indicating that the winner-take-all mechanism is robust. The external inputs to the HVC(RA) neurons are important for extending the working regime. Without it, the working regime is reduced by approximately 50%. The external inputs helps to sustain spike propagation when the inhibition is strong and the excitation is weak [57].

We also investigated spiking profiles of individual neurons during the multiple runs. In Fig. 9(d), we plot spikes of eight selected HVC(RA) neurons and two HVC(I) neurons over five runs. HVC(RA) neurons in the first few groups of the chains spike during both syllables A and B. Other HVC(RA) neurons burst once at precise times during either syllable A or B, but not both. The interneurons spike broadly during both syllables. Although the spikes of HVC(I) neurons are not as sparse as HVC(RA) neurons, their timings have some consistency from run to run because an HVC(I) neuron is connected to a fixed set of HVC(RA) neurons and is most active when these HVC(RA) neurons burst. These firing patterns are very similar to those observed in zebra finch during singing [40], except that HVC(RA) neurons in the first few groups can spike during several different syllables. The bursts of individual neurons, especially those close to branching points, are not as consistent as in the case of zebra finch. This is because the inhibition is strong and the inhibitory neurons are noisy.

To characterize the noisiness of the spikes of HVC(RA) neurons, we computed the unreliability index for each neuron. We computed the probability p of the neuron spiking when the activity propagates to the group that the neuron belongs to. The neuron is most reliable if it spikes or is silent every time, most unreliable if the probability is 0.5. The unreliability can be characterized by the entropy, defined as $-p\log_2 p-(1-p)\log_2(1-p)$. The unreliability index is defined as the entropy normalized by the entropy when $p=0.5$. The index is 0 if $p=1$ or $p=0$; is 1 if $p=0.5$. We computed the unreliability index of all HVC(RA) neurons for each parameter pair in the working regime. The averaged index is roughly a decreasing function of the ratio of the excitation and inhibition, as shown in Fig. 9(e). When the excitation is weak compared to the inhibition, the noisy spiking of the inhibitory neurons can induce noisy responses of HVC(RA) neurons, and the averaged index is high, reaching 0.3 in the worse case (this corresponds to $p=0.95$ or $p=0.05$). When the excitation is sufficiently large compared to the inhibition, HVC(RA) neurons spike more reliably, and the index is around 0.05 (corresponding $p=0.994$ or $p=0.006$). The noise in the external inputs also contributes to these run-to-run fluctuations.

For each parameter pair in the working regime, we also computed the probability of selecting chain A after activity reaches the end of chain A. The probability ranges from 0.3 to 0.9. When the excitation is low compared to the inhibition, the probability is mostly larger than 0.5. This reflects the bias of inhibition to chain B introduced when the connections between HVC(RA) neurons and HVC(I) neurons are randomly set. Increasing the excitation reduces the bias.

The transition probability can be changed by biasing the excitatory connection strengths between the chains or the external inputs to the chains. We systematically varied the maximum excitatory conductance G_{EEmaxA} of the connections from the end to the beginning of chain A, while keeping G_{EEmaxB} of the connections from the end of chain A to the beginning of chain B constant ($0.3\ \mathrm{mS/cm^2}$) [Fig. 10(a)].

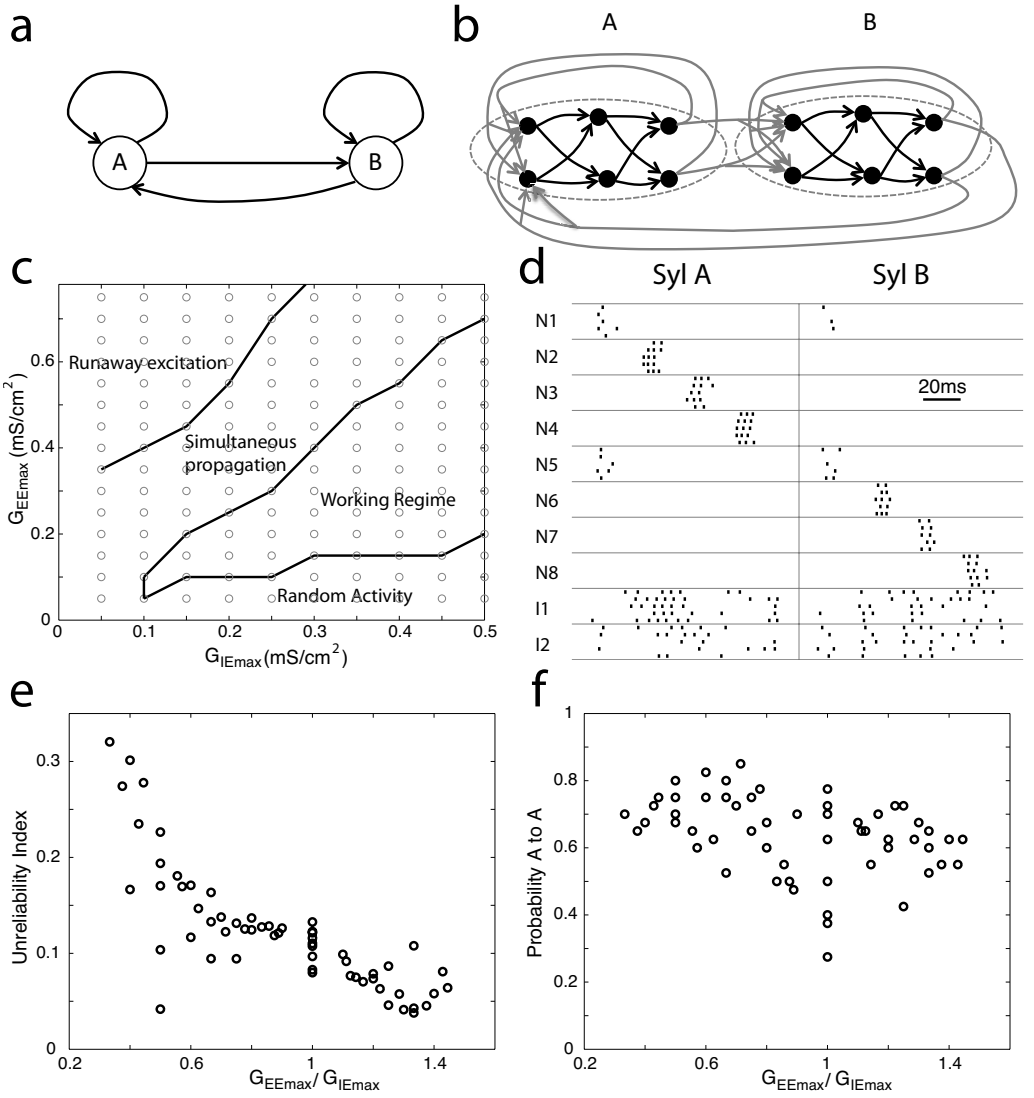

FIG. 9. Multiple runs of the dynamics of a branching chain network corresponding to a simple syntax. (a) The syntax. There are two syllables, A and B. The transition diagram is all-to-all. (b) The schematics of connectivity of the branching chain network of HVC(RA) neurons implementing the syntax. (c) Phase diagram in the space of G_{IEmax} and G_{EEmax}. The diagram is based on 40 simulations on each parameter pair indicated by the gray circle. (d) Spikes of 10 neurons over 5 runs of the dynamics during syllables A and B. Spike of different neurons are separated with gray lines. Here G_{EEmax}=0.3 mS/cm^2 and G_{IEmax}=0.4 mS/cm^2. Neurons $N1$ to $N4$ belong to the chain corresponding to syllable A and $N5$ to $N8$ to syllable B. $I1$ and $I2$ are interneurons. (e) Averaged unreliability index of all HVC(RA) neurons as a function of G_{EEmax}/G_{IEmax}. (f) Probability of selecting syllable A after syllable A as a function of G_{EEmax}/G_{IEmax}.

The probability of selecting chain A as a function of the ratio between G_{EEmaxA} and G_{EEmaxB} is a sigmoidal. It is essentially 0 when the ratio is 0.9, and increases to 1 when the ratio is 1.1. The probability is thus quite sensitive to the changes of the connection strength between the chains. We also systematically varied the level of external inputs by injecting a constant bias excitatory conductance G_b to HVC(RA) neurons in chain A or in chain B [Fig. 10(b)]. When G_b is applied to chain A, the probability of selecting chain A steadily increases with G_b. When G_b is applied to chain B, the probability steadily decreases. Thus, bias in the external levels to the chains substantially changes the transition probabilities.

The transition dynamics between the chains is Markovian. In other words, the transition probabilities from the current chain to others do not depend on the prior dynamics. To demonstrate this point, we simulated spike propagations in the branching chain network shown in Fig. 8 and generated 40 syllable sequences with 99 syllables on average. We computed the probabilities of transitions from a syllable to others. For example, from syllable B, the transition probabilities to syllables A, B, C, and D are 0, 0.495, 0.408, and 0.097, respectively. We then tested whether this transition probability depends on the previous state of the network. For example, the transition probabilities from syllable B when it is preceded by syllable A is 0, 0.485, 0.422, 0.093. The χ^2 test of goodness of fit between these two sets of probabilities, excluding the transition with 0 probability, returned $P=5\times10^{-4}$, indicating that syllable A had no significant effect on the transition probabilities from syllable B. Similarly, χ^2 tests on the effects of preceding syllables to the transition

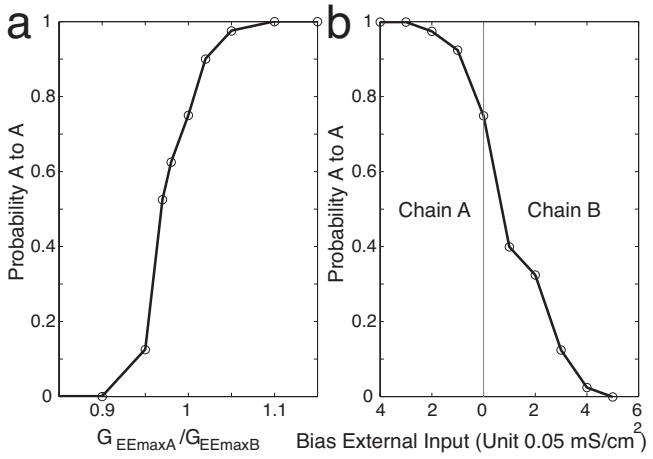

FIG. 10. Probability of transition from chain A to A in the network shown in Fig. 9. (a) The connection strength G_{maxA} from the final group to the first group of chain A is systematically changed relative to $G_{maxB}=0.3$ mS/cm^2, the maximum connection strength from chain A to B. (b) Extra constant external conductance injected to neurons in chain A (left of the vertical line) or in chain B (right).

probabilities from all syllables showed no significance ($P<0.05$). One can also test the Markovian property by studying the probability distributions of subsequences, most conveniently, the frequencies of repeats of a single syllable. For example, the frequency $N(n)$ of observing n consecutive B's is plotted in Fig. 11. If the transitions are Markovian, the distribution is described by an exponential function, i.e., $N(n)=N_0(p_{BB})^n$. Here N_0 is an adjustable parameter, and $p_{BB}=0.495$ is the observed transition probability from B to B. The predicted curved fits well the observed distribution, as shown in Fig. 11 ($P<0.02$, χ^2 test using 1 to 6 repeats).

It is possible that several chains produce the same syllable because HVC to RA connections are learned [44,61,62], and different chains could have very similar connections to the same set of RA neurons [63]. If this is the case, the syllable sequence cannot be described by Markovian model even though the transition dynamics between the chains is Markovian. This effect is shown in Fig. 12. Here, the chain corresponding to D in Fig. 8 now drives syllable C, producing a modified syllable transition rule shown in Fig. 12(a). There are two chains driving the same syllable C. This many-to-one mapping produces a non-Markovian transition between the syllables, as shown in Fig. 12(b). The repeats distribution of syllable C is far from the exponential distribution. The distribution peaks at $n=2$ because the transition between the two chains driving syllable C is pronounced.

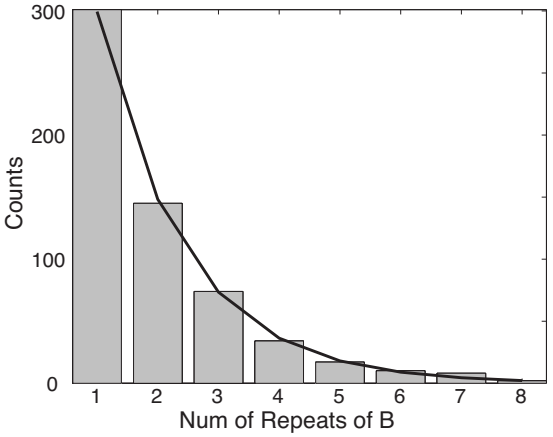

FIG. 11. Distribution of the number of repeats of syllable B in the network shown in Fig. 8. The bars are the counts observed for a given number of repeats. The black line is the fit to the exponential function predicted by the Markov model.

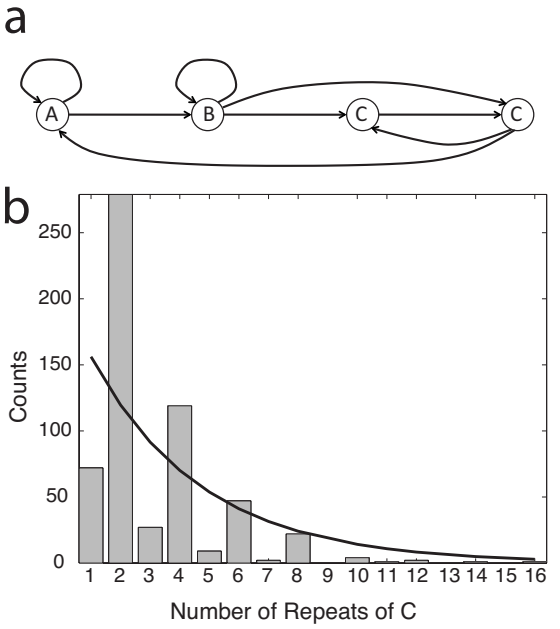

FIG. 12. Distribution of the number of repeats of syllable C in the network shown in Fig. 8 but the chain originally encoded syllable D now encodes syllable C. (a) The modified transition diagram between the syllables. (b) The distribution of the number of repeats of syllable C. The bars are the counts observed for a given number of repeats. The black line is the fit to the exponential function predicted by the Markov model.

IV. DISCUSSION

The song syntax of songbird species such as Bengalese finch contains both restrictions and randomness. A syllable can be followed by one syllable in a restricted set, and the choice is stochastic [13]. In our model, syllables are driven by chain networks of RA-projecting neurons in HVC. The permitted transitions between the syllables are encoded in the branching connection patterns between the chains, and the probabilistic choices of the syllables are enforced by the winner-take-all mechanism mediated by feedback inhibition through the inhibitory interneurons and aided by noise in the neural activity. The transition probabilities are controlled by connection strengths at the branching points as well as the external inputs. Our computational analysis demonstrates that this mechanism is robust and does not require a delicate tuning of the network parameters.

The idea that a syllable is driven by spike propagation in a chain network of HVC(RA) neurons is suggested by recent experimental and computational works on zebra finch, whose

songs consist of fixed sequences of syllables [10]. An HVC(RA) neuron bursts only once at a precise time point during a syllable [40], indicating that distinctive groups of HVC(RA) neurons drive different syllables, and HVC(RA) neurons are activated successively [40,44]. Experiments that cooled HVC during singing further supports that the timings of HVC(RA) bursts are generated within HVC [46]. These observations can be explained by spike propagations on chain networks of HVC(RA) neurons [47,48]. It remains to be seen whether these results in zebra finch can be extended to other species with variable songs, as required in our model.

Inhibition is crucial in our mechanism. Strong inhibition is required to prevent simultaneous propagations of spikes in multiple chains. Random connections between HVC(RA) neurons and HVC(I) neurons provide mutual inhibition among HVC(RA) neurons. Because an HVC(I) neuron is connected by HVC(RA) neurons in multiple chains, it can spike across multiple syllables. Some degree of temporal precision in the spikes of HVC(I) neurons can exist because the HVC(I) neurons are driven by HVC(RA) neurons, which burst with precise timings. These patterns of HVC(I) activity agree with those observed in extracellular recordings of HVC(I) neurons during singing in zebra finch [40] and in Bengalese finch [64]. The microcircuitry of HVC supports the possibility of mutual inhibition between HVC(RA) neurons via HVC(I) neurons [36]. It will be interesting to see whether the inhibition to HVC(RA) neurons is particularly strong in songbird species with variable syllable sequences. Our model predicts that disrupting inhibition should severely impair the song, creating abnormal syllables and syntax due to simultaneous activations of multiple chains. The population activity of HVC(I) neurons is transiently elevated at branching points because of simultaneous activations of several chains before the winner-take-all mechanism selects one chain. Subsequently it decreases since the elevated inhibition quenches the HVC(RA) activity, then it returns to the normal level after the winner-take-all competition is complete. Such transients could be observed in recordings of HVC(I) neurons during singing.

The song control system of songbird is bilaterally organized [20,23,65]. There are no direct connections between the HVCs in the two hemispheres [21,23]. Therefore, HVC(RA) neurons in different hemispheres cannot directly excite or inhibit each other. Our model requires a strong lateralization of the control of song syntax. In particular, all chains encoding syllables in the same set following a syllable must reside in the same hemisphere so that they can be activated through the branching connections and compete through the feedback inhibition via the HVC(I) neurons. If all chains are activated by connections from other chains, the song should be entirely controlled by the HVC in one side. Hemispherical dominance of the control of complex song syntax is supported by lesion studies in canary [20,66] and in Bengalese finch [67], although there is a possibility that some of the effects of the laterization could be peripheral in origin [68,69]. Further experiments are needed to unambiguously address whether the control of complex song syntax resides in one hemisphere.

Recent cooling [46] and stimulation [70] experiments suggest that in zebra finch, the song control is lateralized to one HVC at any given moment, and the control switches back and forth between the two HVCs over time scales comparable to those of syllables. The switch could be through the feedback from RA to HVC through the brainstem and UVA [46,65,71,72]. Thus it is quite possible that the syllable-encoding HVC chains are activated through the feedback loop rather than through direct activations from other chains. If so, the two HVCs could control separate parts of the song syntax. Our model can be easily adapted to use the feedback loop as the chain activation mechanism. Other parts of our model, in particular the winner-take-all mechanism of selecting one of several activated chains for spikes to propagate, should remain the same. It will be interesting to see whether the switching of song control between the two HVCs generalizes to species with complex song syntax.

In our model, HVC(RA) neurons are driven by random excitatory external inputs. The external inputs enhance the robustness of the winner-take-all competition of spike propagations among multiple chain networks [57]. The winner-take-all mechanism requires a strong inhibition to prevent simultaneous spike propagations in multiple chains. However, strong inhibition also tends to stop spike propagations altogether. The external inputs help to prevent such ceasing of activity. We propose that the external inputs come from UVA and/or NIF [21,29–31,73]. Although in our model all chains receive the same amount of external drive, this does not have to be the case. Biases in the external inputs affect the transition probabilities at the branching points. NIF is the major source of auditory input to HVC [25–28]. Distortion of auditory feedback could thus change the transition probabilities between the syllables online by altering the NIF input, as observed in experiments on Bengalese finch [18,64]. Complete removal of auditory input by deafening leads to emergence of novel syllable transitions in Bengalese finch [15,16,18]. An explanation is that deafening alters the NIF inputs to HVC, possibly reducing the biases to the chain networks and also increasing noise, so that previously suppressed transitions can emerge. Removal of NIF reduces the song complexity in Bengalese finch [74]. In our model, this could be due to the reduction of the external inputs and noise with the NIF removal, which makes weak transitions disappear and syllable sequences stereotyped. The transition probabilities of syllables in Bengalese finch differ in songs directed to female compared to songs undirected [75]. This might be due to the state dependent changes of auditory inputs to HVC, as observed in zebra finch [76]. Detailed modeling and comparison with the experiments are needed to fully address the questions on how auditory inputs, NIF, and behavioral states modify complex song syntax.

The transitions between the chain networks in our model can be described by a Markov model. If each chain drives a unique syllable type, the resulting song syntax should be Markovian. However, if multiple chains encode the same syllable type, the song syntax can be non-Markovian. Instead, the syllable sequences should be described by partially observable Markov model (POMM), which is a special case of the hidden Markov model [77]. In POMM, state transitions are Markovian. Each state emits a single symbol, but multiple states can emit the same symbol. The chains in our model correspond to the states, and the syllables correspond

to the symbols. It has been shown that the syntax of Bengalese finch songs is not Markovian; rather, the syntax is better fit with higher order Markov models (although the statistics were not shown), in which state transitions are associated with chunks of syllables, with a syllable possibly appearing in many different chunks [13]. It remains to be seen whether the POMM can statistically describe the complex syllable sequences such as those of Bengalese finch. The many-to-one mapping between the chain networks in HVC and a syllable type is plausible since the connections from HVC to RA are learned [44,61,62], and different sets of HVC(RA) neurons could develop highly similar connection patterns to the same set of RA neurons. Indeed, there is evidence that HVC activity can be different during the vocalizations of the same syllable types [37,68]. An analogous many-to-one mapping from different sets of RA neurons to the same acoustic feature has been shown [43]. Future experiments, perhaps with *in vivo* recordings of HVC(RA) neurons during singing [40], could resolve this issue.

It is possible to make the transitions between the chains non-Markovian by introducing use-dependent biophysical mechanisms such as synaptic depression, spike frequency adaptation, and/or facilitation of inhibition. In zebra finch, the tempo of the motif slows downs as the motif is repeated [78], suggesting that some adaptive process is present. It will be interesting to investigate this possibility further.

We used a two-compartment model with dendrite and soma for HVC(RA) neurons. The dendrite is capable of generating calcium spike with a stereotypical voltage profile, which drives stereotyped burst of sodium spikes in the soma (Fig. 4). The model is motivated by the observation that HVC(RA) neurons in zebra finch emit stereotyped bursts with three to seven spikes within about 6 ms during singing [40]. The model attributes the HVC(RA) burst to an intrinsic cellular mechanism located in the dendrite. Jin *et al.* have shown that dendritic spike enhances the stability of burst propagation in chain networks [47]. The model is supported by recent intracellular recordings of HVC(RA) neurons (Long, Jin, and Fee, submitted). The robustness of the winner-take-all propagation of spikes in branched chain networks does not critically depend on the choice of neuron model. In a recent theoretical work, Chang and Jin [57] studied the winner-take-all propagation mechanism using simple leaky integrate-and-fire neurons and obtained a working parameter regime that is similar to the one shown in Fig. 9(c). The choice of neuron model does introduce some differences. With the leaky integrate-and-fire neurons, the mechanism requires strong external drive; the working regime does not exist without the external drive [57]. With the two-compartment model, the external drive can be absent if the excitation and inhibition are near the boundary that separates the working regime from the simultaneous propagation regime, shown in Fig. 9(C). This difference is due to the enhanced robustness of spike propagation in chain networks with the two-compartment model [47].

To prevent simultaneous spike propagations in multiple chains, the feedback back inhibition between HVC(RA) neurons must be fast enough. In our model, we have not explicitly introduced spike transmission delays. Nonetheless, the feedback inhibition is delayed compared to the direct excitation between HVC(RA) neurons because the inhibition is mediated through HVC(I) neurons. Synchronous spikes in one group of HVC(RA) neurons in a chain evoke spike responses in the connected HVC(I) neurons with latencies ranging from 0.5 to 3.5 ms (mean 1.5 ms, standard deviation 0.8 ms). Paired recordings in HVC slices from zebra finch have shown that HVC(I) neurons mediate fast feedback inhibition [36]. The average response time of an HVC(I) neuron to a single spike from an HVC(RA) neuron was 1.4 ms, as measured by the time for the membrane potential to reach 25% of the peak response value [36]. An HVC(RA) neuron responded to a single spike from an HVC(I) neuron with an averaged response time of 1.7 ms [36]. Thus, the latency of feedback inhibition between HVC(RA) neurons is about 3.1 ms. On surface, the latency is beyond the range in our model. However, two factors must be considered. First, the absolute latency is not important. What matters is how much the feedback inhibition is delayed relative to the direct excitation. Recordings in HVC(RA) neuron pairs found that the averaged response time is 4 ms [36]. Therefore, the feedback inhibition is not much delayed relative to the excitation. Second, the response times were measured in the experiments with single spike inputs [36]. If measured with multiple, synchronous spikes, as in our model, the response times should be shorter. We therefore believe that the latency of feedback inhibition in our model is consistent with the experimental data. We also tested whether our model works when the averaged delay of inhibition is increased to 3 ms by reducing the strengths of the excitatory connections from HVC(RA) neurons to HVC(I) neurons. It does, in a more restricted parameter regime, as long as the overall inhibition strength is maintained by increasing the number of interneurons and the strengths of the inhibitory synapses. Increasing the external drive also helps. Hence, our model can handle increased delay of feedback inhibition. An interesting theoretical question is what new phenomena might emerge with increased delay of feedback inhibition. Chang and Jin observed that the delay can lead to synchronous spiking of nearby groups in the chain networks, creating functional "supergroups," but the winner-take-all propagation does not breakdown [57]. In future this issue should be explored systematically, especially with the two-compartment model of HVC(RA) neurons.

There are alternative mechanisms of generating complex birdsong. Katahira *et al.* proposed a model in which groups of inhibitory interneurons in HVC form branching chain networks [63]. Each group of HVC(I) neurons is mutually connected with a group of HVC(RA) neurons. Sequential activity in HVC(RA) groups is generated by periodic burst inputs from UVA to HVC(RA) neurons and disinhibition of the HVC(RA) groups, a mechanism first suggested by Drew and Abbott [79]. A winner-take-all competition at the branching points is introduced through mutual inhibition. As in our model, the transition dynamics between the chains is Markovian, and non-Markovian syllable sequences is induced using the many-to-one mapping between HVC(RA) neurons and the syllables. In this model, HVC(I) neurons sequentially pause and elevate activity once during the sequence generation in one chain, and is tonically active otherwise. Such activity patterns are not observed in recordings of HVC(I) neurons in both zebra finch [37,40] and Bengalese finch [64].

It is also unclear whether this model can produce bursts of HVC(RA) neurons with millisecond precision relative to the syllables as observed in zebra finch [40].

It is possible that the stochastic decision of sequencing syllables is done outside of HVC. NIF is proposed as the site of syntax control [74]. LMAN (the lateral magnocellular nucleus of the anterior nidopallium), the output of a basal ganglia-forebran circuit in songbirds, has been shown to influence syllable sequence variability in juvenile zebra finch [80,81]. However, recent experiments have demonstrated that LMAN has little effect on syllable sequencing in adult Bengalese finch [82]. Another possibility is MMAN (the medial magnocellular nucleus of the anterior neostriatum), which projects to HVC [83]. To be definitive about syntax control, experiments must be careful in distinguishing the site where the stochastic decisions of selecting syllables are made from sites that simply provide supporting signals.

The songs of songbird species are diverse [84]. Our model of controlling variable syllable sequences, which emphasizes the role of HVC, is constructed by extrapolating from the experimental and modeling works on the zebra finch [40,44,47,48]. It is most likely that the model applies to species such as the Bengalese finch, which is closely related to the zebra finch [13]. Other songbird species could have different or additional mechanisms of controlling syllable sequences. For example, the canary can sing trills with syllable repetition rate greater than 30 syllables per second, during which there is no inspiration [69,85]. The number of syllable repetition in such a trill is limited by the oxygen demand [69]. The roles of physical, metabolic and other constraints on song production should be considered in future models of variable birdsongs.

In conclusion, we have shown that variable syllable sequences can be generated within HVC through competitive spike propagations in chain networks of HVC(RA) neurons connected into branching chain pattern. The feedback inhibition provided by HVC(I) neurons is critical in this process. Our model predicts that syllable sequences can be statistically described with partially observable Markov model.

ACKNOWLEDGMENTS

This research was supported by Sloan Foundation, the Huck Institute of Life Science at the Pennsylvania State University, and NSF Grant No. 0827731. We thank Alexey Kozhevnikov for useful comments and for providing the data in Fig. 1, Joseph Jun and Garrett Evans for useful discussions during the early stages of this work, and Aaron Miller for reading the paper.

APPENDIX

1. Two-compartment model of HVC(RA) neuron

The membrane potentials $V_s(t)$ of the soma obeys the following equation:

$$C_m A_s \frac{dV_s(t)}{dt} = A_s(I_{s,L} + I_{s,\mathrm{Na}} + I_{s,\mathrm{K}dr} + I_{s,exc} + I_{s,inh} + I_{s,ext}) + \frac{(V_d - V_s)}{R_c} \quad \text{(A1)}$$

$C_m = 1\ \mu\mathrm{F/cm^2}$ is the membrane capacitance; $A_s = 5000\ \mu\mathrm{m^2}$ is the area of the somatic compartment; $I_{s,L} = -G_L(V_s - E_L)$ is the leak current, with leak conductance $G_L = 0.1\ \mathrm{mS/cm^2}$ and reversal potential $E_L = -80$ mV; $I_{s,\mathrm{Na}} = -G_{s,\mathrm{Na}} m_\infty^3 h(V_s - E_{\mathrm{Na}})$ is the Na^+ current, with conductance $G_{s,\mathrm{Na}} = 60\ \mathrm{mS/cm^2}$, reversal potential $E_{\mathrm{Na}} = 55\ \mathrm{mS/cm^2}$, Na^+ activation function $m_\infty(V) = 1/\{1 + \exp[-(V_s + 30)/9.5]\}$ and gating variables h; $I_{s,\mathrm{K}dr} = -G_{s,\mathrm{K}dr} n^4 (V_s - E_{\mathrm{K}})$ is the delay-rectified K^+ current, with conductance $G_{\mathrm{K}dr} = 8\ \mathrm{mS/cm^2}$, reversal potential $E_{\mathrm{K}} = -90$ mV, and gating variable n; $I_{s,exc} = -g_{s,exc}(t) V_s$ is the excitatory synaptic current, where $g_{s,exc}(t)$ is the total excitatory synaptic conductance; $I_{s,inh} = -g_{s,inh}(t)(V_s - E_I)$ is the inhibitory synaptic current, where $g_{s,inh}(t)$ is the total inhibitory synaptic conductance, and $E_I = -80$ mV is the reversal potential; and finally, $I_{s,ext}$ is the external current; $R_c = 55\ \mathrm{M\Omega}$ is the coupling resistance between the two compartments.

The synaptic conductance follows a kick-and-decay kinetics:

$$g_{s,exc;s,inh} \rightarrow g_{s,exc;s,inh} + G \quad \text{(A2)}$$

when a spike arrives at an excitatory or inhibitory synapse with conductance G, and

$$\tau \frac{dg_{s,exc;s,inh}}{dt} = -g_{s,exc;s,inh} \quad \text{(A3)}$$

in between spikes. The synaptic time constant τ for both excitatory and inhibitory synapses is set to 5 ms.

The gating variables h, n follow the equation

$$\tau_x \frac{dx}{dt} = x_\infty - x, \quad \text{(A4)}$$

where $x = h, n$. The voltage dependences of the gating variables are $h_\infty = 1/\{1 + \exp[(V_s + 45)/7]\}$; $\tau_h = 0.1 + 0.75/\{1 + \exp[(V_s + 40.5)/6]\}$; $n_\infty = 1/\{1 + \exp[-(V_s + 35)/10]\}$ $\tau_n = 0.1 + 0.5/\{1 + \exp[(V_s + 27)/15]\}$

The equation for the membrane potential $V_d(t)$ of the dendritic compartment is

$$C_m A_d \frac{dV_d(t)}{dt} = A_d(I_{d,L} + I_{d,\mathrm{Ca}} + I_{d,\mathrm{CaK}} + I_{d,exc} + I_{d,inh} + I_{d,ext}) + \frac{(V_s - V_d)}{R_c}, \quad \text{(A5)}$$

where $A_d = 10000\ \mu\mathrm{m^2}$ is the area of the dendritic compartment; $I_{d,L} = -G_{d,L}(V_d - E_L)$ is the leak current, with leak conductance $G_{d,L} = 0.1\ \mathrm{mS/cm^2}$ and reversal potential $E_L = -80$ mV; $I_{d,\mathrm{Ca}} = -G_{\mathrm{Ca}} r^2 (V_d - E_{\mathrm{Ca}})$ is the high threshold Ca^{++} current, with conductance $G_{\mathrm{Ca}} = 55\ \mathrm{mS/cm^2}$, reversal potential $E_{\mathrm{Ca}} = 120$ mV, and gating variable r; $I_{d,\mathrm{CaK}} = -G_{\mathrm{CaK}} c/(1 + 6/[\mathrm{Ca}])(V_d - E_{\mathrm{K}})$ is the calcium-dependent K^+ current, with conductance $G_{\mathrm{CaK}} = 150\ \mathrm{mS/cm^2}$, gating variable c, calcium concentration [Ca], and reversal potential $E_{\mathrm{K}} = -90$ mV; $I_{d,exc}$ and $I_{d,inh}$ are the excitatory and inhibitory synaptic currents, whose dynamics is the same as in the somatic model; and finally, I_{ext} is the external current to the dendritic compartment.

The gating variables r, c follow Eq. (4), with $r_\infty = 1/\{1+\exp[-(V_d+5)/10]\}$; $\tau_r = 1$; $c_\infty = 1/\{1+\exp[-(V_d-10)/7]\}$, $\tau_c = 10$. The calcium concentration obeys the following equation:

$$\frac{d[\mathrm{Ca}]}{dt} = 0.1 I_{d,\mathrm{Ca}} - 0.02[\mathrm{Ca}]. \tag{A6}$$

2. Single compartment model of HVC(I) neuron

The membrane potential $V(t)$ of the inhibitory neuron follows:

$$C_m \frac{dV(t)}{dt} = I_L + I_{\mathrm{Na}} + I_{\mathrm{K}dr} + I_{KHT} + I_{exc} + I_{inh} + I_{ext}, \tag{A7}$$

where $C_m = 1\ \mu\mathrm{F/cm^2}$ is the membrane capacitance; $I_L = -G_L(V-E_L)$ is the leak current, with leak conductance $G_L = 0.1\ \mathrm{mS/cm^2}$ and reversal potential $E_L = -65$ mV; $I_{\mathrm{Na}} = -G_{\mathrm{Na}} m^3 h (V-E_{\mathrm{Na}})$ is the Na^+ current, with conductance $G_{\mathrm{Na}} = 100\ \mathrm{mS/cm^2}$, reversal potential $E_{\mathrm{Na}} = 55\ \mathrm{mS/cm^2}$, and gating variables m, h; $I_{\mathrm{K}dr} = -G_{\mathrm{K}dr} n^4 (V-E_{\mathrm{K}})$ is the delay-rectified K^+ current, with conductance $G_{\mathrm{K}dr} = 20\ \mathrm{mS/cm^2}$, reversal potential $E_{\mathrm{K}} = -80$ mV, and gating variable n; $I_{KHT} = -G_{KHT} w (V-E_{\mathrm{K}})$ is the high threshold K^+ current, with conductance $G_{KHT} = 500\ \mathrm{mS/cm^2}$ and gating variable w; $I_{s,exc} = -g_{exc}(t)V$ is the excitatory synaptic current, where $g_{exc}(t)$ is the total excitatory synaptic conductance; $I_{inh} = -g_{inh}(t)(V_s - E_I)$ is the inhibitory synaptic current, where $g_{inh}(t)$ is the total inhibitory synaptic conductance, and $E_I = -75$ mV is the reversal potential; and finally, I_{ext} is the external current. The dynamics of the excitatory and inhibitory conductance is the same as in the single compartment model of HVC(RA) neuron, except that the time constant of the excitatory conductance τ_{exc} is set to 2 ms.

The gating variables m, h, n are governed by the following equation:

$$\frac{dx}{dt} = \alpha_x(1-x) - \beta_x x, \tag{A8}$$

where $x = m, h, n$. The voltage dependences of the gating variables are $\alpha_m = (V+22)/\{1-\exp[-(V+22)/10]\}$; $\beta_m = 40\exp[-(V+47)/18]$; $\alpha_h = 0.7\exp[-(V+34)/2]$; $\beta_h = 10/\{1+\exp[-(V+4)/10]\}$ $\alpha_n = 0.15(V+15)/\{1-\exp[-(V+15)/10]\}$; $\beta_n = 0.2\exp[-(V+25)/80]$. The gating variable w follows:

$$\tau_w \frac{dw}{dt} = w_\infty - w, \tag{A9}$$

where $w_\infty = 1/[1+\exp(-V/5)]$ and $\tau_w = 1$.

[1] K. S. Lashley, in *Cerebral Mechanisms in Behavior*, The Hixon Symposium, edited by L. A. Jeffress (Wiley, New York, 1951), pp. 112–136.
[2] B. J. Rhodes, D. Bullock, W. B. Verwey, B. B. Averbeck, and M. P. Page, Hum. Mov. Sci. **23**, 699 (2004).
[3] D. A. Rosenbaum, R. G. Cohen, S. A. Jax, D. J. Weiss, and R. van der Wel, Hum. Mov. Sci. **26**, 525 (2007).
[4] J. Tanji, Annu. Rev. Neurosci. **24**, 631 (2001).
[5] B. B. Averbeck, M. V. Chafee, D. A. Crowe, and A. P. Georgopoulos, Proc. Natl. Acad. Sci. U.S.A. **99**, 13172 (2002).
[6] M. Ohbayashi, K. Ohki, and Y. Miyashita, Science **301**, 233 (2003).
[7] W. H. Thorpe, Ibis **100**, 535 (1958).
[8] P. Marler, Am. Sci. **58**, 669 (1970).
[9] K. Immelmann, in *Bird vocalization*, edited by R. Hinde (Cambridge University Press, Cambridge, England, 1969), pp. 61–74.
[10] P. Price, J. Comp. Physiol. Psychol. **93**, 260 (1979).
[11] A. J. Doupe and P. K. Kuhl, Annu. Rev. Neurosci. **22**, 567 (1999).
[12] H. Williams, Ann. N.Y. Acad. Sci. **1016**, 1 (2004).
[13] K. Okanoya, Ann. N.Y. Acad. Sci. **1016**, 724 (2004).
[14] K. Dietrich, Z. Tierpsychol **52**, 5776 (1980).
[15] K. Okanoya and A. Yamaguchi, J. Neurobiol. **33**, 343 (1997).
[16] S. M. Woolley and E. W. Rubel, J. Neurosci. **17**, 6380 (1997).
[17] E. Honda and K. Okanoya, Zoolog Sci. **16**, 319 (1999).
[18] J. T. Sakata and M. S. Brainard, J. Neurosci. **26**, 9619 (2006).
[19] D. Jurafsky and J. H. Martin, *Speech and Language Processing* (Prentice-Hall, New Jersey, 2000).
[20] F. Nottebohm, T. M. Stokes, and C. M. Leonard, J. Comp. Neurol. **165**, 457 (1976).
[21] F. Nottebohm, D. B. Kelley, and J. A. Paton, J. Comp. Neurol. **207**, 344 (1982).
[22] D. S. Vicario and F. Nottebohm, J. Comp. Neurol. **271**, 346 (1988).
[23] J. M. Wild, J. Neurobiol. **33**, 653 (1997).
[24] E. S. Fortune and D. Margoliash, J. Comp. Neurol. **360**, 413 (1995).
[25] G. E. Vates, B. M. Broome, C. V. Mello, and F. Nottebohm, J. Comp. Neurol. **366**, 613 (1996).
[26] P. Janata and D. Margoliash, J. Neurosci. **19**, 5108 (1999).
[27] J. A. Cardin, J. N. Raksin, and M. F. Schmidt, J. Neurophysiol. **93**, 2157 (2005).
[28] M. J. Coleman and R. Mooney, J. Neurosci. **24**, 7251 (2004).
[29] H. Williams and D. S. Vicario, J. Neurobiol. **24**, 903 (1993).
[30] M. J. Coleman, A. Roy, J. M. Wild, and R. Mooney, J. Neurosci. **27**, 10024 (2007).
[31] R. H. Hahnloser, C. Z. Wang, A. Nager, and K. Naie, J. Neurosci. **28**, 5040 (2008).
[32] P. Dutar, H. M. Vu, and D. J. Perkel, J. Neurophysiol. **80**, 1828 (1998).
[33] M. Kubota and I. Taniguchi, J. Neurophysiol. **80**, 914 (1998).
[34] R. Mooney, J. Neurosci. **20**, 5420 (2000).
[35] J. M. Wild, M. N. Williams, G. J. Howie, and R. Mooney, J. Comp. Neurol. **483**, 76 (2005).
[36] R. Mooney and J. F. Prather, J. Neurosci. **25**, 1952 (2005).
[37] A. C. Yu and D. Margoliash, Science **273**, 1871 (1996).
[38] A. S. Dave and D. Margoliash, Science **290**, 812 (2000).

[39] M. S. Brainard and A. J. Doupe, J. Neurosci. **21**, 2501 (2001).
[40] R. H. Hahnloser, A. A. Kozhevnikov, and M. S. Fee, Nature (London) **419**, 65 (2002).
[41] A. Leonardo, Proc. Natl. Acad. Sci. U.S.A. **101**, 16935 (2004).
[42] M. H. Kao and M. S. Brainard, J. Neurophysiol. **96**, 1441 (2006).
[43] A. Leonardo and M. S. Fee, J. Neurosci. **25**, 652 (2005).
[44] M. S. Fee, A. A. Kozhevnikov, and R. H. Hahnloser, Ann. N.Y. Acad. Sci. **1016**, 153 (2004).
[45] A. Kozhevnikov and M. S. Fee, J. Neurophysiol. **97**, 4271 (2007).
[46] M. A. Long and M. S. Fee, Nature (London) **456**, 189 (2008).
[47] D. Z. Jin, F. M. Ramazanoglu, and H. S. Seung, J. Comput. Neurosci. **23**, 283 (2007).
[48] M. Li and H. Greenside, Phys. Rev. E **74**, 011918 (2006).
[49] M. Abeles, *Corticonics* (Cambridge University Press, Cambridge, England, 1991).
[50] M. Abeles, *Local Cortical Circuits: An Electrophysiological Study* (Springer-Verlag, Berlin, 1982), Vol. 18.
[51] W. James, *The Principles of Psychology* [Harvard University Press (reprint 1983), Cambridge, MA, 1890].
[52] D. Hebb, *The Organization of Behavior* (Wiley, New York, NY, 1949).
[53] S. Amari, IEEE Trans. Comput. **C21**, 1197 (1972).
[54] D. Kleinfeld, Proc. Natl. Acad. Sci. U.S.A. **83**, 9469 (1986).
[55] H. Sompolinsky and I. I. Kanter, Phys. Rev. Lett. **57**, 2861 (1986).
[56] J. K. Jun and D. Z. Jin, PLoS ONE **2**, e723 (2007).
[57] W. Chang and D. Z. Jin, Phys. Rev. E **79**, 051917 (2009).
[58] L. Gibb, T. Q. Gentner, and H. D. Abarbanel, J. Neurophysiol. **102**, 1748 (2009).
[59] N. Golding, H. Jung, T. Mickus, and N. Spruston, J. Neurosci. **19**, 8789 (1999).
[60] M. Hausser, N. Spruston, and G. Stuart, *Diversity and Dynamics of Dendritic Signaling* (2000).
[61] K. Doya and T. Sejnowski, in *The New Cognitive Neurosciences*, edited by M. Gazzaniga (The MIT Press, Cambridge, MA, 1999).
[62] I. R. Fiete, M. S. Fee, and H. S. Seung, J. Neurophysiol. **98**, 2038 (2007).
[63] K. Katahira, K. Okanoya, and M. Okada, Biol. Cybern. **97**, 441 (2007).
[64] J. T. Sakata and M. S. Brainard, J. Neurosci. **28**, 11378 (2008).
[65] M. F. Schmidt, J. Neurophysiol. **90**, 3931 (2003).
[66] F. Halle, M. Gahr, and M. Kreutzer, J. Neurobiol. **56**, 303 (2003).
[67] K. Okanoya, M. Ikebuchi, H. Uno, and S. Watanabe, Anim. Cogn. **4**, 241 (2001).
[68] J. S. McCasland, J. Neurosci. **7**, 23 (1987).
[69] R. A. Suthers, J. Neurobiol. **33**, 632 (1997).
[70] C. Z. Wang, J. A. Herbst, G. B. Keller, and R. H. Hahnloser, PLoS Biol. **6**, e250 (2008).
[71] R. C. Ashmore, J. M. Wild, and M. F. Schmidt, J. Neurosci. **25**, 8543 (2005).
[72] R. C. Ashmore, J. A. Renk, and M. F. Schmidt, J. Neurosci. **28**, 2613 (2008).
[73] M. J. Coleman and E. T. Vu, J. Neurobiol. **63**, 70 (2005).
[74] T. Hosino and K. Okanoya, Neuroreport **11**, 2091 (2000).
[75] J. T. Sakata, C. M. Hampton, and M. S. Brainard, J. Neurophysiol. **99**, 1700 (2008).
[76] J. A. Cardin and M. F. Schmidt, J. Neurophysiol. **91**, 2148 (2004).
[77] J. Callut and P. Dupont, in *Grammatical Inference: Algorithms and Applications*, edited by G. Paliouras and Y. Sakakibara (Springer-Verlag, Berlin, Heidelberg, 2004), pp. 77–90.
[78] Z. Chi and D. Margoliash, Neuron **32**, 899 (2001).
[79] P. J. Drew and L. F. Abbott, J. Neurophysiol. **89**, 2697 (2003).
[80] B. P. Olveczky, A. S. Andalman, and M. S. Fee, PLoS Biol. **3**, e153 (2005).
[81] C. Scharff and F. Nottebohm, J. Neurosci. **11**, 2896 (1991).
[82] C. M. Hampton, J. T. Sakata, and M. S. Brainard, J. Neurophysiol. **101**, 3235 (2009).
[83] E. F. Foster and S. W. Bottjer, J. Neurobiol. **46**, 142 (2001).
[84] E. Brenowitz, D. Margoliash, and K. Nordeen, J. Neurobiol. **33**, 495 (1997).
[85] R. Hartley, Respir. Physiol. **81**, 177 (1990).